Available online at www.sciencedirect.com
SCIENCE DIRECT®
Brain Research 990 (2003) 182–194
BRAIN RESEARCH
www.elsevier.com/locate/brainres

Research report

Pharmacological characterization of lysophospholipid receptor signal transduction pathways in rat cerebrocortical astrocytes

Tadimeti S. Rao*, Karen D. Lariosa-Willingham, Fen-Fen Lin, Emma L. Palfreyman, Naichen Yu, Jerold Chun[1], Michael Webb

Merck Research Laboratories, 3535 General Atomics Court, Building 1, San Diego, CA 92121, USA

Accepted 31 July 2003

Abstract

Lysophosphatidic acid (1-acyl-2-lyso-*sn*-glycero-3-phosphate; LPA) and sphingosine-1-phosphate (S1P) are bioactive phospholipids which respectively act as agonists for the G-protein-coupled *lp*A receptors (LPA1, LPA2, and LPA3) and *s1p* receptors (S1P1, S1P2, S1P3, S1P4, and S1P5), collectively referred to as lysophospholipid receptors (lpR). Since astrocytes are responsive to LPA and S1P, we examined mechanisms of lpR signaling in rat cortical secondary astrocytes. Rat cortical astrocyte mRNA expression by quantitative TaqMan polymerase chain reaction (PCR) analysis revealed the following order of relative expression of lpR mRNAs: *s1p3>s1p1>lpa1>s1p2=lpa3≫s1p5.* Activation of lpRs by LPA or S1P led to multiple pharmacological effects, including the influx of calcium, phosphoinositide (PI) hydrolysis, phosphorylation of extracellular receptor regulated kinase (ERK) and release of [^{3}H]-arachidonic acid (AA). These signalling events downstream of lpR activation were inhibited to varying degrees by pertussis toxin (PTX) pretreatment or by the inhibition of sphingosine kinase (SK), a rate-limiting enzyme in the biosynthesis of S1P from sphingosine. These results suggest that astrocyte lpR signalling mechanisms likely involve both Gi- and Gq-coupled GPCRs and that receptor-mediated activation of SK leads to intracellular generation of S1P, which in turn amplifies the lpR signalling in a paracrine/autocrine manner.

Theme: B. Cellular and Molecular Biology
Topic: Neuroglia

Keywords: Lysophospholipid receptor; Lysophosphatidic acid; Sphingosine-1-phosphate; Sphingosine kinase; Astrocyte signalling

1. Introduction

Lysophosphatidic acid (1-acyl-2-lyso-*sn*-glycero-3-phosphate; LPA) and sphingosine-1-phosphate (S1P) are bioactive lysophospholipids (LPs) that are present in the serum in micromolar concentrations, mostly derived from activated platelets, bound to and stabilized by the serum albumin. LPA is produced from deacylation of phosphatidic acid (PA) or reduction of lysophosphatidylcholine and can undergo conversion to PA [27]. S1P is produced by phosphorylation of sphingosine by either membrane-bound or cytosolic sphingosine kinase (SK). S1P undergoes dephosphorylation to sphingosine [32–34]. Both LPA and S1P act by activating their cognate G-protein-coupled lysophospholipid receptors (lpR) to stimulate phospholipase C (PLC), inhibit or activate cAMP in cell-type specific manner, and phosphorylate extracellular signal regulated kinase 2 (ERK 2), Rho kinase, phosphoinositide-3-kinases (PI3K) and glycogen synthase kinase (GSK [9,12,13,16,29,32–34]). These signaling events, mediated via coupling to multiple classes of heterotrimeric G proteins (Gi/o, Gq/11/14, Gs, and G12/13), underlie the pleotropic biological effects of LPR activation, such as chemotaxis, cellular differentiation, survival and growth, and regulation of actin-based cytoskeletal reorganization leading to cell adherence and cell shape changes [3,4,8–10,12,22,28].

The precise roles of lpR in the central nervous system are beginning to emerge. For example, LPAR activation leads to (a) norepinephrine release [24], (b) tyrosine phosphorylation

* Corresponding author. Kalypsys, Inc., 11099 North Torrey Pines Road, La Jolla, CA 92037, USA. Tel.: +1-858-754-3300.
E-mail address: trao@kalypsys.com (T.S. Rao).
[1] Current address: The Scripps Research Institute, Department Molecular Biology, 10550 North Torrey Pines Road, La Jolla, CA 92037, USA.

0006-8993/$ - see front matter © 2003 Elsevier B.V. All rights reserved.
doi:10.1016/S0006-8993(03)03527-3

of focal adhesion kinase in the hippocampus [5], (c) increases in intracellular calcium ($[Ca]_i^{+2}$), reduction of cAMP and release of arachidonic acid (AA) in striatal astrocytes [25], (d) induction of neurotrophic factor gene expression and mitogenesis in astrocytes [35], (e) decreased glutamate and glucose uptake in astrocytes [15], (f) regulation of neuroblast morphology [8], and (g) sustained elevation of $[Ca]_i^{+2}$ and induction of hippocampal neuronal death [15]. Similarly, SIP is known to be involved in the nerve growth factor-mediated neuronal survival and differentiation [6], release of glial cell line-derived neurotrophic factor (GDNF) from astrocytes [38], apoptosis of cultured hippocampal neurons [23], induction of Rho-dependent neurite retraction [28], proliferation of astrocytes [26,38], and expression of early growth response-1 and fibroblast growth factor-2 in astrocytes [31].

The lysophospholipid receptors are widely distributed throughout the central nervous system, both in neurons and glia (astrocytes, microglia, and oligodendrocytes [2–5,8–11,19,23,25,26,28,35,39,40,42]. The distribution of lpRs in glial cells and neurons provides an unique opportunity for neuron–glia cross-talk. Diverse external stimuli including growth factors and neurotransmitters, second messengers such as cAMP and ATP, and rise in intracellular calcium levels can affect lysophospholipid biosynthesis, release and lpR activation [33,34], therefore setting a stage for neuronal–glia interactions. It is believed that such autocrine/paracrine regulation of lpR signaling may have important functional consequences in CNS function (see Discussion).

Our laboratory has investigated the lpR distribution and function in glial cells. These results on oligodendrocytes [42] and microglia [17,36] are published elsewhere. The present investigation focuses on the distribution and function of lpRs in astrocytes. The range of pharmacological effects of both LPA and S1P on astrocytes suggests the presence of functional receptors and that these glial cells represent a useful model system to study lpR pharmacology. As a comparative pharmacological characterization of LPAR and S1PR in astrocytes has not been conducted, we examined (1) distribution of lpR mRNA and (2) lpR signal transduction events: (a) ERK2 phosphorylation (b) AA release, (c) PI hydrolysis, and (3) activation of SK in lpR signaling. These results demonstrate a differential distribution of lpR transcripts, marked similarities in signal transduction pathways following activation of lpRs by cognate ligands, and a unique cross-talk between LPAR and S1PR receptor signaling involving downstream activation of SK.

2. Materials and methods

Stock solutions of LPA (10 mM), SIP (500 μM; both from Avanti Polar Lipids, Alabaster, AL) and DL-threo-dihydrosphingosine (DHS; 10 mM; BioMol, Plymouth Meeting, PA), a cell-permeable, competitive inhibitor of sphingosine kinase [20,21,41] were prepared using 1 mg/ml solution of fatty acid-free bovine serum albumin (FAFBSA; Sigma, St. Louis, MO) in distilled water as the vehicle, stored at −70 °C until use, and diluted into tissue culture medium (DMEM; Gibco, Gaithersburg, MD) with glutamine [2 mM] and 1 mg/ml FAFBSA, herein after referred to as TCM). At these concentrations, the LPA stock solution was clear, while the stock solutions of both S1P and DHS remained cloudy. Stock solutions of the MEK1 and MEK2 inhibitor, U-0126 ([1,4-diamino-2,3-dicyano-1,4-bis(2-aminophenylthio)butadiene]; 10 mM), a phosphotidylinositol-3-kinase (PI3K) inhibitor, wortmanin (10 mM) and MAPK inhibitor, PD-98059 (2′-amino-3′-methoxyflavone; 10 mM; all from Calbiochem, San Diego, CA) were prepared in dimethylsulfoxide (DMSO) and stored at −70 °C until use. Stock solutions of the phospholipase C inhibitor, U-73122 ({1-[6-((17-b-methoxyestra-1,3,5-(10)-trien-17-yl)-amino)hexyl]-1*H*-pyrrole-2,5-dione); 10 mM; Calbiochem or Alexis, San Diego, CA) were prepared freshly in DMSO. All stock solutions were diluted into TCM prior to application to astrocyte cultures. Appropriate vehicle controls were included in each experiment. Stock solutions of pertussis toxin (PTX; List Biologicals, Campbell, CA) solutions were prepared in distilled water (1 mg/ml) and stored at 4 °C. In pharmacological experiments, PTX was routinely applied to astrocytes for 18–24 h in a serum-free medium (DMEM with 2 mM Gln) at a final concentration of 200 ng/ml.

2.1. Secondary astrocyte cultures

Primary cerebrocortical mixed glial (astrocytes, microglia, and oligodendrocytes) cultures were prepared from neonatal Sprague–Dawley rat brains (1–2 days old). Whole brains, minus cerebellum, were mechanically dissociated by serial trituration with a fire-polished narrow bore Pasteur pipette. The cells were sedimented by centrifugation (1000 × *g* for 5 min), resuspended in a medium containing DMEM (Gibco) with 25mM glucose and 2mM L-glutamine supplemented with 10% heat-inactivated FBS (Omega Scientific, CA), seeded at a density of 750,000 cells/well in 75-cm^2 flasks (Falcon) (precoated with poly-L-lysine) and incubated at 37 °C in an atmosphere with 5% CO_2 at 95% humidity. The culture medium was changed 6 days later (DIV7) and twice a week thereafter. In these cultures, immature oligodendrocytes (O-2A progenitors) appear as phase-dark process-bearing cells overlying a confluent bed of phase-light astrocytes. After 10–14 days in cultures, astrocytes were separated from O-2A progenitors and microglia by shaking the cultures as per McCarthy and DeVellis [18] (350 rpm, 37 °C, overnight) and replated to assay plates pre-coated with poly-L-lysine. These ‘purified’ or ‘secondary’ astrocyte cultures were used in all biochemical experiments 3–5 days after replating (>97% astrocytes). Twenty four hours before the experiments, cells washed twice and changed to a serum-free medium (DMEM with 2mM Gln) overnight in a tissue culture incubator. Radioactive tracers for biochemical experiments were added at the time of changing the medium.

2.2. Distribution of lpR mRNA in secondary astrocytes: TaqMan PCR analysis

2.2.1. Isolation of total RNA and reverse transcription

Total RNA from adult rat whole brain was isolated using ToTally RNA™ kit (Ambion). For further removal of genomic DNA contamination, total RNA was treated with RNase-free DNase I on RNeasy® midi columns and purified according to RNeasy® Protect Midi kit (Qiagen). Total RNA from rat astrocytes was isolated using RNeasy® Protect Mini kit (Qiagen). One microgram of total RNA was reverse transcribed using RETROscript™ kit (Ambion). In each reverse transcription reaction, a reaction omitting reverse transcriptase was included for the assessment of genomic DNA contamination.

2.2.2. Cloning, construction, and DNA sequencing of mini genes for lpR and β-actin

The cDNA encoding *lp*A1, *lp*A3, *s1p*1, *s1p2*, *s1p3*, *s1p*4, *s1p5*, and β-actin were amplified from rat brain with polymerase chain reaction (PCR) techniques. Primers used for these genes were designed from sequences in the Genebank database (Table 1). For cloning of *lp*R mini genes, 2 μl of cDNA was amplified using 10 pmol of each primer and 25 μl of TaqMan® Universal PCR Master Mix, in a total volume of 50 μl. PCR was performed using a GeneAmp® 9700 thermocycler (ABI) with incubation at 50 °C for 2 min, 95 °C for 10 min, followed by 40 cycles of 15 s at 95 °C and 1 min at 60 °C. The β-actin mini gene was amplified with 2.5 U of *PfuTurbo*® DNA polymerase (Stratagene), 200 nM dNTP, and 10 pmol of each primer, in a total volume of 50 μl for 30 cycles in GeneAmp® 9700 thermocycler (ABI). Each cycle consisted of 30 s at 95 °C, 30 s at 55 °C and 45 s at 75 °C.

The PCR-amplified fragments were subcloned into PCR cloning vectors, pCR®-BluntII-TOPO® or pCR®II-TOPO® (Invitrogen) using PCR Cloning Kit (Invitrogen) (Table 1). The integrity of these genes was confirmed by sequencing using an ABI 3100 automated fluorescence sequencer. The sequence was analyzed using software Sequencher.

Table 1
Sequences of primers and probes, PCR products, and constructs of mini genes

Gene	Accession number	Forward primer (F)/TaqMan probe(TM)/Reverse primer (R) and Forward primer (F)/Reverse primer (R)	Mini genes and fragment size
lpa1	AF090347	F: 5′ GACACCATGATGAGCCTTCTGA	pCR-Blunt II-rLPA1
		TM: 5′ AAAGGCACCCAGCACAATGACCACA	
		R: 5′ CCCGGAGTCCAGCAGACA	
		F: 5′ AGCTGCCTCTACTTCCAGCC	176 bp
		R: 5′ CGCAGACAGTGATGCCCAGT	
lpa3	AF097733	F: 5′ CACACGAGTGGCTCCATCAG	pCRII-TOPO-rLPA3
		TM: 5′ CTCCTAAGACAGTCATCACCGTCTTCATTAGCTTC	
		R: 5′ GGTCCAGCACACCACGAA	
		F: 5′ GGCCTTCTTCATCATGGTGG	
		R: 5′ CATGACGGAGTTGAGCAGCG	274 bp
s1p1	U10303	F: 5′ CTGACCTTCCGCAAGAACATCT	pCR2.1-TOPO-rLPB1
		TM: 5′ CAAGGCCAGCCGCAGTTCCG	
		R: 5′ CTTCAGCAAGGCCAGAGACTTC	
		F: 5′ GAAGTTCCACCGGCCCATGT	
		R: 5′ GGAGATGTTCTTGCGGAAGG	505 bp
s1p2	AF022138	F: 5′ GCCTTGTACGTCCGAATCTACTTC	pCR2.1-TOPO-rLPB2
		TM: 5′ TAGTCCGCTCAAGCCATGCGGAC	
		R: 5′ AGCGTCTGAGGACCAGCAA	
		F: 5′ GTCTGGACCATCTGGAGGCT	
		R: 5′ GTCTGAGGACCAGCAACGTC	169 bp
s1p3	AF184914	F: 5′ ACGCGCGCATCTACTTCCT	pCR-Blunt II-rLPB3
		TM: 5′ CCACCCTGCGGCTGCTGGACT	
		R: 5′ TGGATCTCTCGGAGTTGTGGTT	
		F: 5′ GACGCCAACAAGAAGCACCG	168 bp
		R: 5′ GCTGATGAGAAAGGCAATGTA	
s1p5	AF233649	F: 5′ CTCTAGAGCGCCACCTTACCAT	pCRII-TOPO-rLPB4
		TM: 5′ CAGGCGGCCACCGCCATC	
		R: 5′ CCCAGCAGCAGCGACAA	
		F: 5′ GCCTATGTGCTCTTCTGCGT	
		R: 5′ CAACGACCGTGGCGTGTG	171 bp
βactin	V01217	F: 5′ ATGCCCCGAGGCTCTCTT	
		TM: 5′ CCTTCCTTCCTGGGTATGGAATCCTGTG	
		R: 5′ CTTCATGATGGAATTGAATGTAGTTTC	
		F: 5′ GCTATGAGCTGCCTGACGGT	pCR-Blunt II-rβActin
		R: 5′ GTACTTGCGCTCAGGAGGAG	296 bp

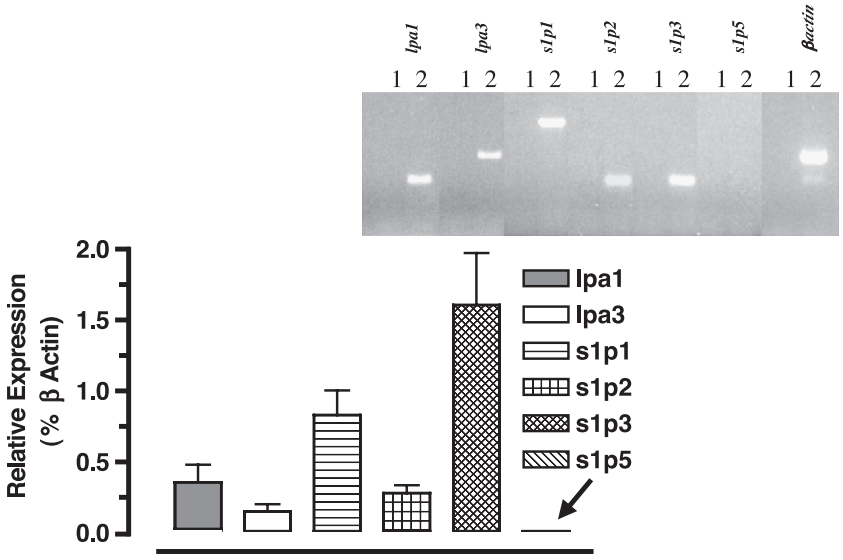

Fig. 1. Inset: RT-PCR detection of mRNA of lpR in rat astrocytes. Lane 1. PCR reaction involving astrocyte cDNA with the omission of reverse transcriptase reaction for the assessment of genomic DNA contamination, Lane 2. PCR reaction with cDNA with the inclusion of reverse transcriptase reaction. Quantitative analysis of mRNA transcripts for lpR in rat cortical astrocytes by TaqMan PCR technique. Primers used specific to each gene and amplified product sizes were listed in Table 1. Data represent expression of individual lpR mRNA relative to β-actin whose expression was normalized to 100. Values represent means ± S.E.M., $n = 3$.

2.2.3. PCR

PCR was performed using 3.0 μl of cDNA samples with 2.5 U of *PfuTurbo*® DNA polymerase (Stratagene), 200 nM dNTP, and 10 pmol of each primer, in a total volume of 50 μl for 30 cycles in GeneAmp® 9700 thermocycler (ABI). Each cycle consisted of 30 s at 95 °C, 30 s at 55 °C and 45 s at 75 °C. Aliquots of amplified samples (15 μl) were assessed by agarose gel electrophoresis.

2.2.4. TaqMan PCR

TaqMan PCR was carried out using an ABI Prism 7900 sequence detector on 1 μl of cDNA samples using 900 nM each primer, 250 nM TaqMan probe, and 25 μl of TaqMan® Universal PCR Master Mix, in a total volume of 50 μl. PCR was executed with incubation at 50 °C of 2 min, 95 °C for 10 min, followed by 40 cycles of 15 s at 95 °C and 1 min at 60 °C. Additional reactions were performed on each 96-well

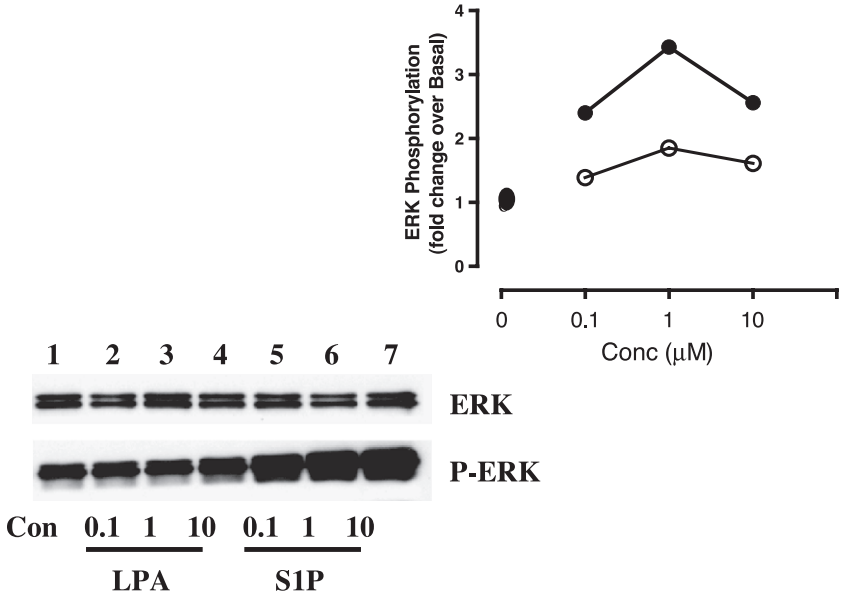

Fig. 2. Western blot analysis of ERK phosphorylation in rat cortical astrocytes upon exposure to S1P (0.1, 1, and 10 μM) and LPA (0.1, 1, and 10 μM) for 10 min. LPA and S1P increase ERK phosphorylation. Data represent results from a typical experiment and replicated in two additional experiments. Inset shows data combined from individual experiments.

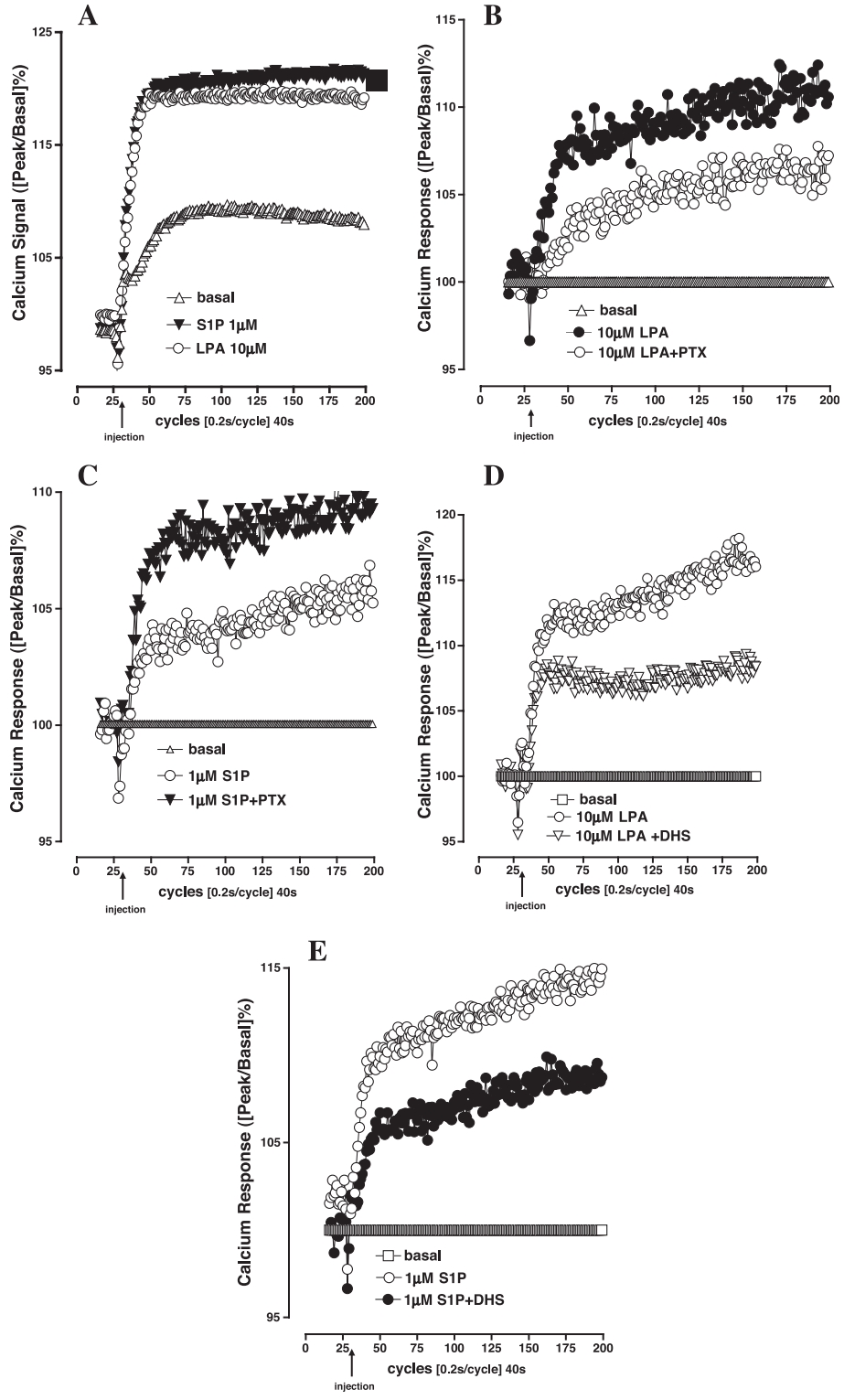

Fig. 3. Regulation of calcium signaling in astrocytes by lpR activation. Both LPA and S1P increase intracellular calcium in cultured astrocytes. Changes in intracellular calcium were measured by fluorimetric analysis of cells loaded with Fluo-4 AM. LPA (10 μM; Panel A and B) and S1P (1 μM; Panel A) increase intracellular calcium. Pretreatment of astrocytes with pertussis toxin (PTX; 200 ng/ml, 18–24 h) significantly attenuated LPA-evoked influx of calcium (Panel B; $p < 0.05$; two-way ANOVA) with no attenuation seen in S1P-induced response (Panel C). Pretreatment with dihydrosphingosine (DHS; 60 μM; 20 min) attenuated increases in intracellular calcium in response to LPA (Panel D) and S1P (Panel E) application ($p < 0.05$; two-way ANOVA). Values represent mean ± S.E.M. ($n = 3$ experiments each with three replicates).

plate using a known dilution of DNA from mini genes as PCR template for constructing a standard curve relating threshold cycle to cDNA concentration. Data were analyzed using software SDS2.0. All measured PCR products were normalized to the amount of β-actin cDNA, and all data were normalized to β-actin and expressed as % β-actin using software Prism 3.0.

2.2.5. Measurement of [Cai^{2+}] by Fluo-4AM using fluorescence plate reader

Intracellular calcium measurements by Fluo-4AM (Molecular Probes, Eugene, OR) were performed, as per Manning and Sontheimer [17] with minor modifications. Astrocytes grown in 48-well plates were washed with assay buffer (20 mM HEPES-buffered EBSS (Gibco) + 10 μM glycine + 40 μM probenecid) and incubated with Fluo-4-AM (10 μM in assay buffer; 100 μl/well) for 2 h at 32 °C. After the dye was removed, cells were washed gently with 500 μl of assay buffer to remove any dye nonspecifically associated with the cell surface and incubated with 100 μl of assay buffer containing 0.1% fatty acid-free BSA in the FLUOstar™ Galaxy (BMG Lab Technologies, Cary, NC) plate carrier at room temperature for 15 min for de-esterification of intracellular AM ester. Test reagents (100 μl, 2 × concentration) were delivered to cultured astrocytes in assay buffer containing 0.1% fatty acid-free BSA and fluorescence intensities were measured for 40 s after which, F_{max} and F_{min} calibrations for quantitative Ca^{2+} measurements were performed. Data were expressed as peak/basal ratio by plotting changes in Ca^{2+} (peak) as a function of time (cycles [0.2 s/cycle]) calibrated relative to the basal Ca^{2+} levels.

2.2.6. Western blot analysis of ERK phosphorylation

Astrocytes were washed with TCM (2–3 × 0.5 ml), exposed for 10 min to LPA or S1P with or without co-treatments, the medium was aspirated off, rinsed once with 4 ml Earle's balanced salt solution and lysed with 300 μl of NP-40 lysis buffer a containing protease inhibitor cocktail (Sigma; NaF, 10 mM; Na_3VO_4, 1 mM and PMSF, 1 mM). Protein levels were determined using bicinchoninic acid (Pierce, Rockford, IL) with bovine serum albumin as the standard. Samples of cell lysates containing equal amounts of protein were subjected to electrophoresis on a 4–20% Tris–HCl Criterion Precast Gel (Bio-Rad, Hercules, CA) and transferred to Hybond ECL nitrocellulose membrane (Amersham Pharmacia Biotech, Piscataway, NJ) by electroblotting. Blots were washed in Tris-buffered saline containing Tween-20 (TBST) containing nonfat dairy milk powder, incubated in p44/42 MAP kinases (Erk1/2) or phosphospecific (Thr202/Tyr204) p44/p42 MAP kinases (pErk1/pErk2) antibodies (1:1000; Cell Signaling, Beverly, MA) at room temperature for 2 h or 4 °C overnight. Blots were washed and incubated with a horseradish peroxidase (HRP)-conjugated goat anti-rabbit IgG as the secondary antibody (1:10,000, Amersham Pharmacia Biotech; 2 h at room temperature), washed again, and processed for immunoreactivity by signal amplification using SuperSignal® West Femto Maximum Sensitivity Substrate (Pierce) and by exposing the blots to Kodak BIOMAX ML film for visualization. Densitometry of immunoblots was used to quantify changes in ERK phosphorylation.

2.2.7. [^{3}H]-arachidonic acid release

Astrocytes in 24-well culture plates were labeled with [^{3}H]-AA ([5,6,8,9,11,12,14,15] [^{3}H]-arachidonic acid; Amersham; 0.166 μCi/ml; 0.5 ml/well; 18–24 h at 37 °C), extensively washed first with warm (37 °C) DMEM (3 × 0.5 ml) and later with TCM (3 × 0.5 ml). After the final wash, pharmacological treatments were applied in TCM. The experiments were terminated by the collection of supernatants following a 20-min incubation at 37 °C in a tissue culture incubator, lysing the cells in Triton-X-100 (0.1%) containing TCM. Radioactivity in supernatants and lysates was determined by liquid scintillation counting, and the data were expressed as fractional efflux.

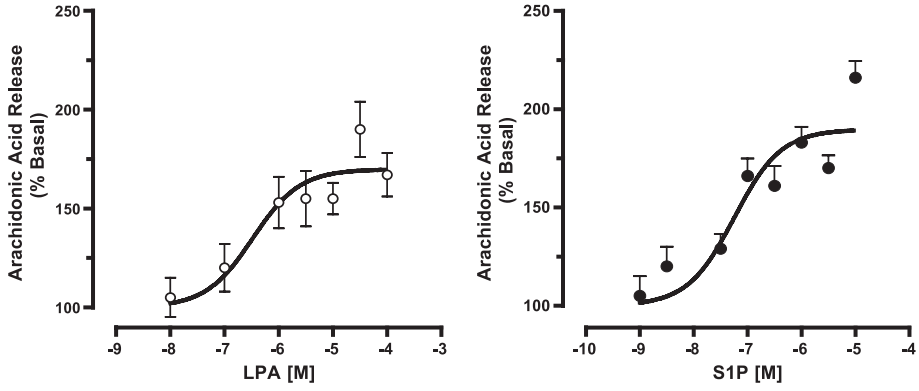

Fig. 4. LPA and S1P increase [^{3}H]-arachidonic acid (AA) release from rat cortical astrocytes. Following overnight labeling with AA, cells were extensively washed and exposed to LPA or S1P for 20 min. Values represent AA release expressed as a percentage of fractional efflux seen under control conditions (mean ± S.E.M., $n = 3–4$ experiments each with 2–3 replicates).

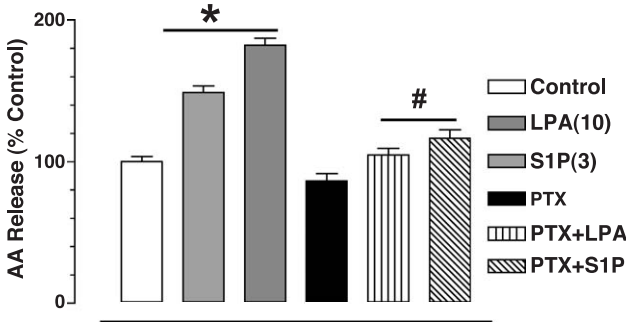

Fig. 5. LPA (10 μM) and S1P (3 μM)-induced AA release in astrocytes is sensitive to inhibition by pretreatment with PTX (200 ng/ml; 18–24 h). Data represent fractional efflux observed with LPA or S1P expressed as a percentage of fractional efflux seen with respective control response (mean ± S.E.M., $n=3–4$ experiments each with 2–3 replicates). *$p<0.05$ vs. control, $^{\#}p<0.05$ vs. no PTX condition (ANOVA followed by Neuman–Keuls test).

2.2.8. PI hydrolysis

Astrocytes grown in 24-well plates were labeled with [^{3}H]-myo-inositol (1 μCi/well) in DMEM with glutamine (0.5 ml/well; 18–24 h at 37 °C), washed with TCM (3 × 0.5 ml), exposed for 30 min to TCM containing LiCl (10 mM) and finally exposed for 60 min to various pharmacological treatments in TCM containing Li in a tissue culture incubator. Following the removal of supernatants, cellular lipids were extracted with cold solvent mixture (HCl [4N]: chloroform–methanol [2:100:200; v:v:v; 0.95 ml/well]), and the extracts were transferred to glass tubes to which equal volumes (0.3 ml) of water-saturated chloroform and chloroform were added. After vortex-mixing and centrifugation, aliquots of the aqueous phase (0.5 ml) were added to exchange resin columns (AG 1-X8; 100–200 mesh formate form) for separation of [^{3}H]-inositol-containing compounds. [^{3}H]-Inositol monophosphate was eluted into scintillation vials and measured by liquid scintillation counting. Aliquots of organic phase (0.5 ml) were dried and counted to determine total [^{3}H]-myoinositol incorporated into cellular lipids and to normalize fractional conversion to inositol monophosphate (IP1).

2.2.9. Statistics

All values are expressed as mean ± standard error of mean (S.E.M., $n=3–6$ individual experiments each with two to three replicates). Data were analyzed by analysis of variance (ANOVA) followed by post hoc analysis (Neuman–Keuls test; Prizm 3.0; GraphPad, San Diego, CA) and statistical significance determined at a $p<0.05$.

3. Results

3.1. Distribution of lpR mRNA in astrocytes

RT-PCR revealed expression of mRNAs for *lpa1*, *lpa3*, *s1p1*, *s1p2* and *s1p3* in rat astrocytes (Fig. 1; inset). Quantitative analysis by TaqMan PCR techniques indicated s1p3 mRNA to be the most abundant *lpR* species in rat astrocytes, followed by *s1p1>lpa1>s1p2=lpa3* (Fig. 1). In contrast, the rat astrocytes contained relatively undetectable levels of mRNA for s1p5, and this pattern is consistent with an exclusive distribution of s1p5 in oligodendrocytes [13]. Similarly, the pattern of distribution of s1p mRNAs in the present study is consistent with the detection mRNAs for *s1p1* and *s1p3* in cultured mouse striatal astrocytes using RT-PCR analysis [26].

3.2. ERK phosphorylation

Initial studies in glial cultures indicated that both LPA (10 μM) and S1P (10 μM) increased ERK activation as measured by increased phosphorylation of p42/p44 MAPK with a peak effect at 10 min (data not shown). LPA and SIP (both at 0.1, 1, and 10 μM) increased phosphorylation of p42/p44 MAPK (Fig. 2). LPA- and SIP-induced ERK phosphorylation was sensitive to pretreatment with a MEK inhibitor, PD-98059 (data not shown). In addition, S1P- and

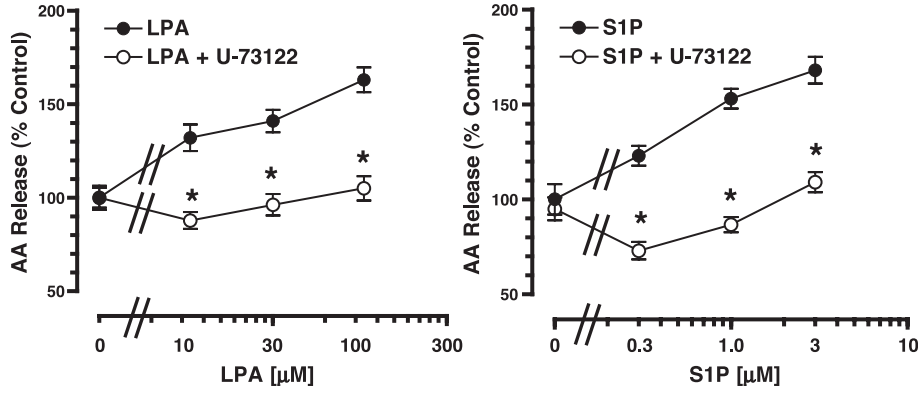

Fig. 6. LPA- and S1P-induced AA release in astrocytes is sensitive to inhibition by pretreatment with the PLC inhibitor, U-73122 (30 μM; 20 min). Data represent fractional efflux observed with LPA or S1P expressed as a percentage of fractional efflux seen with respective control response (mean ± S.E.M., $n=3–4$ experiments each with 2–3 replicates), *$p<0.05$ vs. no U-73122 condition.

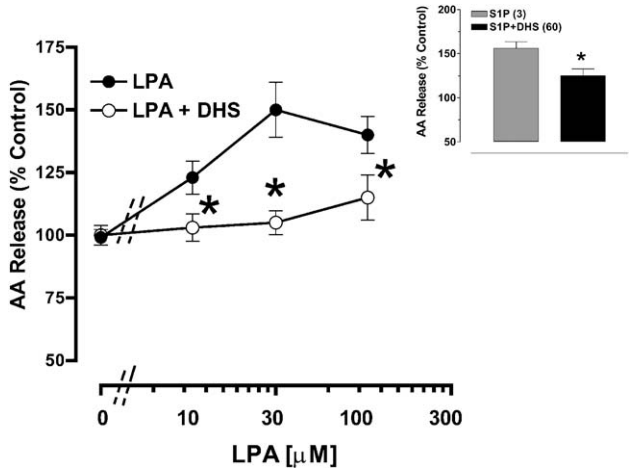

Fig. 7. LPA- and S1P-induced AA release in astrocytes is sensitive to inhibition by pretreatment with the competitive SK inhibitor, DHS (60 μM; 20 min). Data represent fractional efflux observed with LPA or S1P expressed as a percentage of fractional efflux seen with respective control response (mean ± S.E.M., $n = 3–4$ experiments each with 3 replicates), *$p < 0.05$ vs. no DHS condition (ANOVA followed by Neuman–Keuls test or *t*-test).

LPA-induced ERK phosphorylation was greatly attenuated by pretreatment with PTX (data not shown).

3.3. Calcium signaling in astrocytes

Both LPA (10 μM) and S1P (1 μM) increased $[Ca]_i^{+2}$ in rat cortical astrocytes (Fig. 3A) with a rapid increase followed by a period of sustained elevation lasting for up to 40 s after agonist application. Since these $[Ca]_i^{+2}$ measurements reflected population responses, kinetic differences among the individual cells, if any, could not be differentiated. Agonist-induced rapid increases, but not the sustained elevation in $[Ca]_i^{+2}$, persisted in the absence of external calcium and inclusion of 2 mM ethylene glycol-bis-(β-aminoethyl ether)-*N*,*N*,*N*′,*N*″-tetraacetic acid ethylene glycol (EGTA; data not shown). This suggests that internal calcium stores contributed to the rapid increase, whereas the influx of external calcium contributed to the sustained elevation of in $[Ca]_i^{+2}$. Pretreatment of astrocytes with PTX (200 ng/ml; overnight) selectively blunted LPA (10 μM)-induced increases in $[Ca]_i^{+2}$ without affecting the response to S1P (1 μM; Fig. 3B and C). In addition, pretreatment of astrocytes with DHS (60 μM; 20 min), a cell-permeable sphingosine kinase (SK) inhibitor, also blunted both LPA (10 μM) and S1P (1 μM)-induced increases in $[Ca]_i^{+2}$, implicating a role for SK in calcium signaling (Fig. 3D and E).

3.4. AA release

Activation of lpR by both SIP and LPA increased AA release in a concentration-dependent manner. While S1P and LPA were equally efficacious (maximal release; mean ± S.E.M., 195 ± 15 and 170 ± 10, $p > 0.05$), SIP was nearly fivefold more potent than LPA in increasing AA release from astrocytes (EC_{50} [nM], mean ± S.E.M. [3–4]; 57 ± 12 and 333 ± 60, $p < 0.05$; Fig. 4). These potency differences are in agreement with those reported in mouse striatal astrocytes [23,24].

Pretreatment of astrocytes with PTX (200 ng/ml) significantly attenuated both LPA and SIP-evoked arachidonic acid release to near control levels ($p < 0.05$; Fig. 5). This concentration of PTX is known to completely attenuate agonist-induced adenylate cyclase activation/inhibition in cultured systems (data not shown). In cultured mouse striatal astrocytes, LPA-evoked AA release was reported to be relatively resistant to inhibition by PTX pretreatment [23], suggesting involvement of Gq, but not Gi-coupled G-proteins. It is unclear if species differences, i.e., rat vs. mouse, account for the differential PTX-sensitivity.

With a view to further exploring the pharmacology of LPA and S1P-evoked AA release, inhibitors of signal

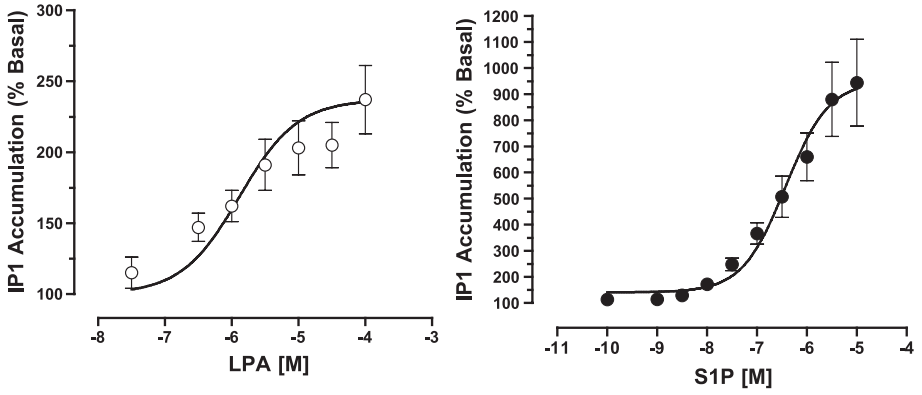

Fig. 8. Concentration-dependent increases in phosphoinositide hydrolysis in cortical astrocytes following activation of lpR with LPA or S1P. Astrocytes were incubated overnight with [^{3}H]-myoinositol to label lipid pools, washed, preincubated in lithium-containing buffer prior to exposure to agonists in lithium-containing buffer for 1 h. Values represent PI hydrolysis expressed as a percentage of basal IP1 accumulation seen under control conditions (mean ± S.E.M., $n = 3–4$ experiments each with 2–3 replicates).

transduction pathways that are known to be downstream to lpR activation were employed. The PLC inhibitor, U-73122 (30 μM), completely abrogated both LPA- and S1P-evoked AA release from astrocytes (Fig. 6). The inhibition of MAPK pathway by PD-98059 (10 μM), Akt pathway by wortmanin (1 μM) or MEK pathway by U-0126 (0.3 μM) did not affect LPA-evoked AA release (data not shown) arguing for a minimal role for these pathways in AA release. Interestingly, pretreatment of astrocytes with DHS, a cell-permeable SK inhibitor, markedly attenuated both LPA- and S1P-evoked AA release (Fig. 7).

3.5. Activation of PLC pathway: PI hydrolysis

Both LPA and S1P increased PI hydrolysis in a concentration-dependent manner demonstrating that lpR activation triggers stimulation of the PLC pathway. S1P was nearly fivefold more efficacious than LPA (maximum responses, mean ± S.E.M. [$n=4$], 944 ± 166% and 237 ± 24%, respectively, $p<0.05$) and threefold more potent than LPA (EC_{50} values, mean ± S.E.M. [$n=3$–4], 375 ± 85 and 1350 ± 200 nM, respectively; $p<0.05$; Fig. 8).

PTX pretreatment significantly attenuated both LPA- and S1P-induced PI hydrolysis (~ 50% in both cases, $p<0.05$; Fig. 9). To investigate the role of PKC in lpR-induced PLC activation, the effect of chelerythrine, a PKC inhibitor, was examined. Pretreatment of astrocytes with chelerythrine (10 μM) completely abrogated both SIP- and LPA-induced PLC activation leading to PI hydrolysis (Fig. 10).

Since inhibition of SK by DHS (60 μM) attenuated both LPA- and SIP-induced calcium signaling and AA release, and since AA release was sensitive to PLC inhibition, we hypothesized that SK activation may also influence the PLC pathway. To test this hypothesis, we examined effects of DHS on lpR-mediated PI hydrolysis. DHS pretreatment attenuated both LPA- and S1P-evoked PI hydrolysis responses by 50% and 40%, respectively ($p<0.05$), suggesting that lpR-induced PLC activation is also subject to modulation by SK (Fig. 11).

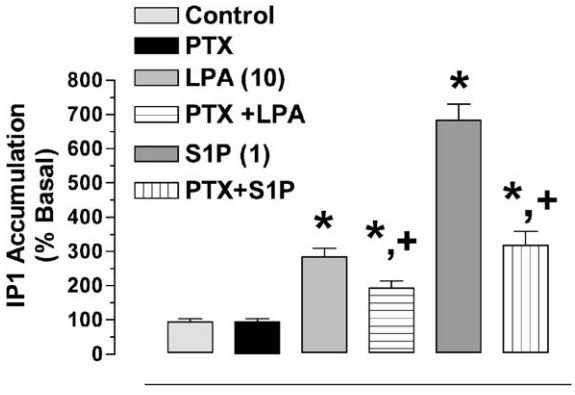

Fig. 9. LPA (10 μM) and S1P (1 μM)-induced PI hydrolysis in astrocytes is sensitive to inhibition by pretreatment with PTX (200 ng/ml; 18–24 h). Data represent fractional IP1 accumulation observed with LPA or S1P expressed as a percentage of IP1 accumulation seen with respective control response (mean ± S.E.M., $n=3$–4 experiments each with 3 replicates), *$p<0.05$ vs. control, $^{+}p<0.05$ vs. no PTX condition (ANOVA followed by Neuman–Keuls test).

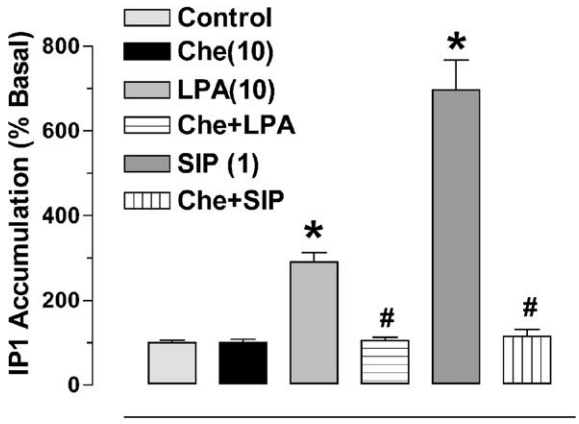

Fig. 10. LPA (10 μM) and S1P (1 μM)-induced PI hydrolysis in astrocytes is sensitive to inhibition by pretreatment with the PKC inhibitor, chelerythrine (Che, 10 μM; 20 min pretreatment). Data represent fractional IP1 accumulation observed with LPA or S1P expressed as a percentage of IP1 accumulation seen with respective control response (mean ± S.E.M., $n=3$–4 experiments each with 3 replicates), *$p<0.05$ vs. control, $^{\#}p<0.05$ vs. no Che condition (ANOVA followed by Neuman–Keuls test).

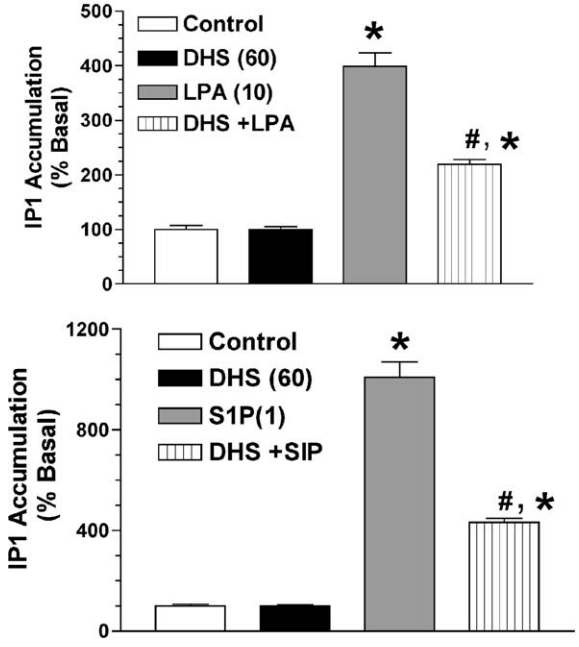

Fig. 11. LPA (10 μM) and S1P (1 μM)-induced PI hydrolysis in astrocytes is sensitive to inhibition by pretreatment with the competitive SK inhibitor, DHS (60 μM; 20 min pretreatment). Data represent fractional IP1 accumulation observed with LPA or S1P expressed as a percentage of IP1 accumulation seen with respective control response (mean ± S.E.M., $n=3$–4 experiments each with 3 replicates), *$p<0.05$ vs. control, $^{\#}p<0.05$ vs. no DHS condition (ANOVA followed by Neuman–Keuls test).

4. Discussion

The main goals for this investigation were to determine the expression pattern of genes encoding lpRs and to investigate the signal transduction mechanisms of lpR in rat cerebrocortical astrocytes. Expression patterns of mRNA for *lpa1*, *lpa3*, *s1p1*, *s1p2*, *s1p3*, and *s1p5* were documented, along with investigation of the role of Gi- and Gq-coupled GPCRs in lpR-induced calcium signaling, AA release, and PI hydrolysis. Most interestingly, the present investigation provides evidence for the activation of sphingosine kinase (SK) as a key common effector mechanism downstream of lpR activation.

4.1. Distribution of lpR mRNA in astrocytes

Two families of related genes *lpa1*, *lpa2*, and *lpa*3 and *s1p1*, *s1p2*, *s1p3*, *s1p4*, and *s1p5* encode for LPAR and S1PR, respectively [9,10,22,29,32,33]. It is also known that both families show 40–50% intra-family sequence identity and 30–35% inter-family identity, and both families in turn are related to the cannabinoid receptors [9,11,12]. In the present investigation, we examined gene expression profile of *lpa* and *s1p* mRNA. TaqMan PCR technique was used to examine the relative quantitative patterns of lpR mRNA expression. The mRNA for *lpa1* is the most abundant of the two LPA species examined (*lpa1* and *lpa3*), while *s1p3* was the most abundant of all lpR species followed by *s1p1*. Rat sequences for *lpa2* and *s1p4* are unknown, and therefore, the expression of these mRNAs was not investigated. We confirmed that mRNA for *s1p5*, reported to be exclusively expressed in oligodendrocytes [13,42], was not detected in astrocytes. Recently Tabuchi et al. [35], using Northern analysis, reported abundant expression of *lpa1* mRNA in cultured rat astrocytes with a lower level of expression in cultured rat neurons. Results from the present investigation, in addition to confirming the above findings, extend these by the detection of low abundance of *lpa3.* The presence of small but detectable levels of *lpa3* mRNA in astrocytes is consistent with a presence of this transcript in perinatal rodent brain [4]. The detection of *lpa1* mRNA in cultured astrocytes contrasts with detection of *lpa1* mRNA by in situ hybridization in adult rat brain oligodendrocytes, but not in astrocytes [11], and with immunohistochemical detection of *lpa1* in oligodendrocytes, but not in astrocytes either in situ or in culture [2]. These discrepancies may be related to increased sensitivity of the quantitative TaqMan PCR technique over the others and/or to induction of *lpa1* in cultured astrocytes, or may reflect the induction of these transcripts following isolation in culture.

4.2. ERK phosphorylation

Consistent with literature reports which established ERK phosphorylation as a key signaling event downstream of lpR activation in several cellular systems [9,14,16,22,25,29], LPA and S1P increased ERK phosphorylation in cultured astrocytes. The sensitivity of lpR-mediated responses to PD98059, a well-known MEK inhibitor, implies that ERK phosphorylation is downstream of lpR-induced MAPK activation. In addition, the sensitivity of this response to PTX implies involvement of Gi-coupled GPCRs. MAPK activation and subsequent ERK phosphorylation are intimately linked to proliferative responses in target cells. Indeed, lpR activation is known to induce proliferative response in cultured astrocytes [25,26,35,38].

4.3. Calcium signaling in astrocytes

Both LPA and S1P increased intracellular calcium. Interestingly, LPA-induced but not S1P-induced response was sensitive to pretreatment with PTX. These results implicate distinct coupling to heterotrimeric G protein subunits. LpR-induced elevations in $[Ca]_i^{+2}$ were sensitive pretreatment with DHS, a cell-permeable SK inhibitor. Since SK is the rate-limiting enzyme in the conversion of sphingosine to SIP, these results suggest lpR-activated SIP generation in astrocytes. The role of SK in lpR signaling was further explored and substantiated both in AA release and PLC activation.

4.4. Arachidonic acid release and activation of PLC pathway

Both LPA and S1P increased PI hydrolysis and AA release in a concentration-dependent manner, and these two signaling responses were PTX sensitive, implying that lpR activation leads to stimulation of the PLC and PLA2 pathways via Gi-coupled GPCRs. In a number of cellular systems, increases in intracellular calcium via PLC-IP3 pathway activate PLA2 enzyme leading to AA release. Therefore, the inhibition of lpR-evoked AA release by PLC inhibitor U-73122 supports a proximal PLC activation step in the events leading to AA release. In contrast, inhibition of MAPK pathway by PD-98059 (10 μM), Akt pathway by wortmanin (1 μM) or MEK pathway by U-0126 (0.3 μM) did not affect LPA-evoked AA release arguing for a minimal role for these pathways in AA release. The lack of effect of PD-98059 on LPA-evoked AA release was in contrast with the sensitivity of LPA-induced ERK phosphorylation and suggests divergent mechanisms. Several lines of evidence suggest a cross-talk between GPCR-induced activation of phospholipase C and protein kinase C (PKC) pathways: (a) activation of PKC by diacylglycerol, a by-product of PLC activation, and (b) downregulation of the PLC pathway via feedback inhibition by prior activation of protein kinase C by phorbol esters or by inhibition of PKC pathway by agents such as staurosporine or chelerythrine [7]. The inhibitory effects of chelerythrine on PI hydrolysis are consistent with the notion that PKC activation precedes PLC activation. These results are also in agreement with the attenuation of lpR-stimulated PI hydro-

lysis in cultured mouse striatal astrocytes by phorbol ester-induced PKC activation [25,26]. In addition, these results indicate that lpR activation leads to stimulation of PKC, PLA2, and PLC pathways. The inhibition of SK by DHS attenuated both LPA- and SIP-induced AA release and PI hydrolysis. These observations suggest that lpR-mediated SK activation also influences PLA2 and PLC pathways.

4.5. Multiple lpRs in astrocytes and signaling redundancy

The overall pharmacological profiles of LPA and S1P in astrocytes should reflect that a mixture of individual receptors encoded by these genes. The consequences of lpR activation by cognate ligands were very similar in that activation of LPARs by LPA or S1PRs by S1P resulted in (a) elevation of intracellular calcium, (b) ERK-phosphorylation, and (c) arachidonic acid release and PI hydrolysis. It is unclear if these pharmacological responses are subtype specific or represent a collective activation of lpR. Activation of individual members of lpRs in recombinant systems led to overlapping downstream transduction events, perhaps reflective of shared G protein-coupling [9,16]. Of the heterotrimeric GPCRs, only Gi-coupled GPCR responses show PTX sensitivity. In recombinant systems, S1P1R couple only to Gi, whereas both S1PR2 and S1PR3 couple to Gi, Gq, and G13. Therefore, activation of these receptors by S1P results in inhibition or, in some cases, activation of adenylate cyclase, ERK phosphorylation, and PLC activation. Predictably, these diverse responses show varying degrees of PTX sensitivity. The profile of S1P-mediated responses in astrocytes is consistent with the involvement of multiple members of S1PR family. Similarly, activation by LPA of LPA1, LPA2, and LPA3 receptors stably expressed in a neuronal cell line (B-103), results in increases in AA release, ERK phosphorylation in a PTX sensitive manner, and activation of PLC pathway in a PTX-insensitive manner, implicating involvement of Gi and Gq, respectively, in these pathways [14]. These results show both similarities and differences with those seen in cultured astrocytes. These differences may arise due in part to the well-known cell-type specific GPCR coupling for lpRs [16,32,33]; for example, LPA activates MAPK pathway in oligodendrocytes in a relatively PTX-insensitive manner [42], which contrasts with complete PTX sensitivity in cultured astrocytes [25].

The presence of multiple lpR in astrocytes with shared or similar signaling properties raises interesting issues of signaling selectivity and consequences of ligand activation. Since the endogenous ligands LPA and S1P do not exhibit marked subtype selectivity, activation of lpR by LPA or S1P may result in a downstream signaling redundancy. However, this redundancy may allow for signal summation for fine-tuning biological responses. In addition, emerging evidence supports homo- and heterodimerization of lpRs in recombinant systems [37], and if this were to occur in vivo, such a phenomenon may further modify cellular responses to ligand activation.

4.6. Role of sphingosine kinase in lpR signaling

A major source of calcium signaling via GPCRs involves PLC-IP3 dependent calcium release from intracellular stores. However, in a number of experimental systems, PLC-IP3-independent calcium mobilization by GPCRs has been documented [20,21]. Some of the examples include (1) calcium mobilization via M2 muscarinic cholinergic receptors in HEK-293 cells [20,21] and (2) LPA-induced calcium signaling in SHSY-5Y neuroblastoma cells in the complete absence of IP3 production [41]. Such a process is now known to involve activation of SK, leading to an enhanced production of S1P. S1P, in turn, can further amplify calcium signaling through its effects on endoplasmic reticulum. DL-threo-dihydrosphingosine (DHS) is a competitive, cell-permeable SK inhibitor, and sensitivity of pharmacological responses to DHS is taken as an evidence in favor of in situ SK activation [6,20,21,41]. LPA-induced calcium signaling in SHSY-5Y cells was found to be DHS sensitive, implying SK activation, and this was confirmed by LPA-induced generation of [^{3}H]-S1P from [^{3}H]-sphingosine [41]. In addition, in cell lines stably expressing recombinant S1P1, S1P3, or S1P5 receptors, activation by S1P resulted in the generation of intracellular S1P in a PTX-sensitive manner, implicating receptor-mediated generation [21]. Since astrocytes contained both functional LPRs and S1PRs, we hypothesized that lpR activation may trigger SK activation. Consistent with the hypothesis, our studies revealed that agonist-induced AA release, PLC activation, and calcium signaling all are sensitive to varying degrees to DHS, suggesting that activation of SK is a consequence of lpR activation.

Activation of SK as an event subsequent to lpR activation has several implications. First, intracellular generation of S1P can further amplify signaling via the endoplasmic reticulum. Second, since SK is also membrane bound [1], the potential exists for local signal amplification via extracellular S1P generation. More importantly, influx of calcium via multiple mechanisms, such as the activation of GPCRs, depolarization, and ionophore application is known to activate SK [20,21,41]. These observations suggest that SK activation is an important cellular response to calcium signaling and posit that physiologic neurotransmission via GPCR and ion channels has the potential to generate S1P locally as novel autocrine/paracrine tertiary messenger. The magnitude of S1PR activation following such diverse stimuli is likely to be tightly controlled by regulated degradation of S1P to sphingosine by S1P-phosphatase.

4.7. Roles of lpR in physiology and pathology

The precise roles of astrocytic lpRs in in vivo physiology are unclear. Astrocytes not only provide nutrient support to neurons, but emerging evidence points to an active role of astrocytes in CNS repair following injury [30]. In addition, astrocytes, in concert with endothelial cells, form the

blood–brain barrier. Therefore, the presence of cognate receptors for lpR on neurons, endothelial cells, and glia, including astrocytes, invoke pleotropic actions of LPA and S1P on these cells. The presence of micromolar concentrations of LPA and S1P in serum and the presence of calcium-activated SK as a common downstream event all suggest a role in central nervous system development, remodeling, injury and repair, and blood–brain barrier function. The frontal hematomas observed in lpa1 (− / −) and lpa1 (− / −)/lpa2(− / −) embryos suggest that lpRs are critical regulators of blood–brain barrier permeability and/or vascular reactivity under both physiological and pathophysiological conditions [39,40]. Similarly, expression analyses suggest potential roles for lpRs in neurogenesis, angiogeneis, survival/apoptosis, and neural signaling [19,34,39,40].

References

[1] N. Ancellin, C. Colmant, J. Su, Q. Li, N. Mitterder, S.-S. Chae, S. Stefansson, G. Liau, T. Hla, Extracellular export of sphingosine kinase-1 enzyme, J. Biol. Chem. 277 (2002) 6667–6675.

[2] P. Cerevera, M. Tirard, S. Barron, J. Allard, S. Trottier, J. LaCombe, C. Dumas-Duport, P. Sokoloff, Immunohistological localization of myelinating cell-specific receptor LPA1, Glia 38 (2002) 126–136.

[3] J. Chun, Lysophospholipid receptors: implications for neural signaling, Crit. Rev. Neurobiol. 13 (1999) 151–168.

[4] J.J.A. Contos, J. Chun, The mouse lpA3/Edg7 lysophosphatidic acid receptor gene: genomic structure, chromosomal localization, and expression pattern, Gene 267 (2001) 243–253.

[5] P. Dirkenderen, J. Siciliano, M. Toutnat, J.A. Girault, Differential regulation of FAK+, PYK2/Cakβ, two related tyrosine kinases in rat hippocampal slices: effects of LPA, carbachol, depolarization and hyperosmolarity, Eur. J. Neurosci. 10 (1998) 1667–1675.

[6] L.C. Edsall, G.G. Pirianov, S. Spiegel, Involvement of sphingosine-1-phosphate in nerve growth factor-mediated neuronal survival and differentiation, J. Neurosci. 17 (1997) 6269–6952.

[7] E. Edwards, C.R. Ashby, R.Y. Wang, Further characterization of 5-HT- and 5-HT3 receptor agonists'-stimulated phosphoinositol phosphates accumulation, Brain Res. 617 (1993) 113–119.

[8] N. Fukushima, J.A. Weiner, J. Chun, Lysophosphatidic acid (LPA) is a novel extracellular regulator of neuroblast morphology, Dev. Biol. 228 (2000) 6–18.

[9] N. Fukushima, I. Ishii, J.J.A. Contos, JA. Weiner, J. Chun, Lysophospholipid receptors, Ann. Rev. Pharmacol. Toxicol. 41 (2001) 507–534.

[10] E.J. Goetzl, S. An, Diversity of cellular receptors and functions for the lysophospholipid growth factors lysophosphatidic acid and sphingosine-1-phosphate, FASEB J. 12 (1998) 1589–1598.

[11] J.H. Hecht, J.A. Weiner, S.R. Post, J. Chun, Ventricular zone gene-1 (vzg-1) encodes a lysophosphatidic acid receptor expressed in neurogenic regions of the developing cerebral cortex, J. Cell Biol. 135 (1996) 1071–1083.

[12] T. Hla, M.-J. Lee, N. Ancellin, J.H. Paik, M.J. Kluk, Lysophospholipids—receptor revelations, Science 294 (2001) 1875–1878.

[13] D.-S. Im, C.E. Heise, N. Ancellin, B.F. Dowd, G.J. Shei, R.P. Heavens, M.R. Rigby, T. Hla, S. Mandala, G. McAllister, S. George, K.R. Lynch, Characterization of a novel sphingosine-1-phosphate receptor, edg 8, J. Biol. Chem. 275 (2000) 14281–14286.

[14] I. Ishii, J.J.A. Contos, N. Fukushima, J. Chun, Functional comparisons of the lysophosphatidic acid receptors, LPA1/VZG-1/EDG-2, lpA2/EDG-4 and LPA3/EDG-7 in neuronal cell lines using a retrovirus expression system, Mol. Pharmacol. 58 (2000) 895–902.

[15] J.N. Keller, M.R. Steiner, M.P. Mattson, S.M. Steiner, Lysophosphatidic acid decreases glutamate and glucose uptake by astrocytes, J. Neurochem. 67 (1996) 2300–2305.

[16] M.J. Kluk, T. Hla, Signaling of sphingosine-1-phosphate via S1P/Edg-family of G-protein-coupled receptors, Biochim. Biophys. Acta 1582 (2002) 72–80.

[17] F.-F. Lin, C.-S. Tham, M.E. Williams, T.S. Rao, M. Webb, Acutely isolated microglia display different gene expression profiles from cultured and LPS-activated microglia, Soc. Neurosci. Abstr. (448.3).

[18] T.J.J. Manning, H. Sontheimer, Recording of intracellular Ca^{2+}, Cl^{-}, pH and membrane potential in cultured astrocytes using a fluorescence plate reader, J. Neurosci. Methods 91 (1999) 73–81.

[19] K.D. McCarthy, J. DeVellis, Preparation of separate astroglial and oligodendroglial cultures from rat cerebral tissue, J. Cell Biol. 85 (1980) 890–902.

[20] C. McGiffert, J.J.A. Contos, B. Friedman, J. Chun, Embryonic brain expression analysis of lysophospholipid receptor genes suggests roles of *S1P1* in neurogenesis and *S1P1-3* in angiogenesis, FEBS. Lett. 531 (2002) 103–108.

[21] D. Meyer zu Heringdorf, H. Lass, R. Alemany, K.T. Laser, E. Neumann, C. Zhang, M. Schmidt, U. Rauen, K.H. Jacobs, C.J. van Koppen, Sphingosine kinase-mediated Ca^{+2} signaling by G-protein-coupled receptors, EMBO J. 17 (1998) 2830–2837.

[22] D. Meyer zu Heringdorf, H. Lass, I. Kuchar, M. Lipinski, R. Alemany, U. Rumenapp, K.H. Jacobs, Stimulation of intracellular sphingosine-1-phosphate production by G-protein-coupled sphingosine-1-phosphate receptors, Eur. J. Pharmacol. 414 (2001) 145–154.

[23] W. Moolenaar, Bioactive lysophospholipids and their G protein-coupled receptors, Exp. Cell Res. 253 (1999) 230–238.

[24] A.N. Moore, A.W. Kampfl, X. Zhao, R.L. Hayes, P.K. Dash, Sphingosine-1-phosphate induces apoptosis of cultured hippocampal neurons that require protein phosphatases and activator protein-1 complexes, Neuroscience 94 (1999) 405–415.

[25] T. Nishikawa, Y. Tomori, S. Yamashita, S.I. Shimuzu, Inhibition of Na^{+}, K^{+}-ATPase activity by phospholipase A2 and several lysophospholipids; possible role of phospholipase A2 and noradrenaline release from cerebral cortical synaptosomes, J. Pharm. Pharmacol. 41 (1989) 450–458.

[26] A. Pebay, Y. Torrens, M. Toutant, J. Cordiaer, J. Glowinski, M. Tence, Pleotropic actions of lysophosphatidic acid on astrocytes, Glia 28 (1999) 25–33.

[27] A. Pebay, M. Toutant, J. Premont, C.-F. Calvo, L. Venance, J. Cordier, J. Glowinski, M. Tence, Sphingosine-1-phosphate induces proliferation of astrocytes: regulation by intracellular signaling cascades, Eur. J. Neurosci. 13 (2001) 2067–2076.

[28] M.-F. Pages, P. Simon, J.S. Valet, J. Saulnier-Blache, Lysophosphatidic acid synthesis and release, Prostaglandins Other Lipid Mediat. 64 (2001) 1–10.

[29] F.R. Postma, K. Jalink, T. Hengeveld, W.H. Moolenaar, Sphingosine-1-phosphate rapidly induces Rho-dependent neurite retraction: action through a specific cell surface receptor, EMBO J. 15 (1996) 2388–2392.

[30] S. Pyne, N.J. Pyne, Sphingosine-1-phosphate signaling in mammalian cells, Biochem. J. 348 (2000) 385–402.

[31] J.L. Ridet, S.K. Malhotra, A. Privat, F.H. Gage, Reactive astrocytes: cellular and molecular cues to biological function, Trends Neurosci. 20 (1997) 570–577.

[32] K. Sato, K. Ishikawa, M. Ui, F. Okajima, Sphingosine-1-phosphate induces expression of early growth response-1 and fibroblast growth factor-2 through a mechanism involving extracellular signal regulated kinase in astroglial cells, Brain Res. Mol. Brain Res. 72 (1999) 182–189.

[33] S. Siehler, D.R. Manning, Pathways of transduction engaged by sphingosine-1-phosphate through G-protein-coupled receptors, Biochim. Biophys. Acta 1582 (2002) 94–99.

[34] S. Spiegel, S. Milstein, Functions of a new family of sphingosine-1-phosphate receptors, Biochim. Biophys. Acta 1484 (2000) 107–116.
[35] S. Spiegel, S. Milstein, Sphingosine-1-phosphate: an enigmatic signaling lipid, Nat. Rev. Mol. Biol. 4 (2003) 397–407.
[36] S. Tabuchi, K. Kume, M. Aihara, T. Shimuzu, Expression of lysophosphatidic acid receptor in rat astrocytes: mitogeneic effect and expression of neurotrophic genes, Neurochem. Res. 25 (2000) 573–582.
[37] J.R. Van Broklyn, B. Behbahmi, N.H. Lee, Homodimerization and heterodimerization of S1P/EDG sphingosine-1-phosphate receptors, Biochim. Biophys. Acta 1582 (2002) 89–93.
[38] K. Yamagita, M. Tagami, Y. Torri, F. Takenaga, S. Tsumagari, S. Itoh, Y. Yamori, Y. Nara, Sphingosine-1-phosphate induces the production of glial cell line-derived neurotrophic factor and cellular proliferation in astrocytes, Glia 41 (2003) 199–206.
[39] X. Ye, N. Fukushima, M.A. Kingsbury, J. Chun, Lysophosphatidic acid in neural signaling, NeuroReport 13 (2002) 2169–2175.
[40] X. Ye, I. Ishi, M.A. Kingsbury, J. Chun, Lysophosphatidic acid as a novel cell survival/apoptotic factor, Biochim. Biophys. Acta 1585 (2002) 108–113.
[41] K.W. Young, M.D. Bootman, D.R. Channing, P. Lipp, P.R. Maycox, J. Meakin, R.A. Challis, S.R. Nahorski, Lysophosphatidic acid-induced Ca^{+2} mobilization requires intracellular sphingosine-1-phosphate production, J. Biol. Chem. 275 (2000) 38532–38539.
[42] N. Yu, K.D. Lariosa, F.-F. Lin, M. Webb, T.S. Rao, Characterization of lysophosphatidic acid and sphingosine-1-phosphate-mediated signal transduction in rat cortical oligodendrocytes, Glia (2003) (in press).